A New Metastable Phase in Rapidly Solidified Al-Zr Alloys

T. OHASHI AND R. ICHIKAWA

IT has been previously shown that the solid solubility of zirconium in aluminum could be extended from the equilibrium value of 0.27 wt pct to 1 ~ 1.1 wt pct by chill casting an Al-Zr alloy into a water-cooled copper mold and that the solute of zirconium which could not dissolve in aluminum turned up as a secondary phase in the primary α solid solutions when the concentration of zirconium was higher than that of the extended solid solubility.[1,2] On photomicroscopic observations, it could be seen that there was a difference in shape between the secondary phases as shown in Fig. 1; *i.e.*, the one was formed by rapid solidification and the other by slow solidification.

The·present work was aimed at clarifying the crystal structure of these phases.

Specimens were prepared from Al-5.39 wt pct Zr alloys containing 0.17 wt pct Fe, 0.050 wt pct Si, 0.002 wt pct Cu, and 0.009 wt pct Ti and thin plate castings of the alloys (1 by 20 by 40 ~ 50 cu mm^3) were made by using a water-cooled copper mold to obtain a high cooling rate. The constituents in these alloys were identified by X-ray diffraction analysis with nickel filtered Cu-Kα radiation using a Debye-Scherrer camera of 114.6 mm diam and a JEOL diffractometer. Two shapes of specimen for this analysis were prepared from the thin plate castings. The one was a sheet polished electrolytically and the other was powdery crystals which were separated chemically from the thin plate castings by a method described by Hollingsworth *et al.*[3] In addition to the above analysis, transmission electron microscopic observations (on a JEM 200Å, 200kv) were carried out with the thinned specimens of Al-3 wt pct Zr alloys cast into the same copper mold as mentioned above.

X-ray diffraction lines from the separated crystals, some of which were annealed at various temperatures for 30 min, are shown in Fig. 2. In case of no heat treatment, the diffraction lines from the separated crystals and/or the secondary phase in the sheet-shaped specimens could be indexed as cubic structure having a lattice constant of 4.0731 ± 0.0008Å. The observed diffraction lines from such an unknown phase are summarized and compared with those calculated for cubic ordered and fcc structures in Table I. After a number of trial-and-error procedures, the crystal structure of this phase has been solved to have the cubic ordered structure of $L1_2$ type on the supposition that its composition is based on the formula Al_3Zr.

After annealing above a temperature of 510°C, on the other hand, it could be seen that several weak diffraction lines appeared in X-ray films and their intensities increased with increasing annealing temperature. These diffraction lines corresponded to those from the Al_3Zr having a tetragonal structure (DO_{23} type) which is stable up to the melting point of 1580°C.[4-6]

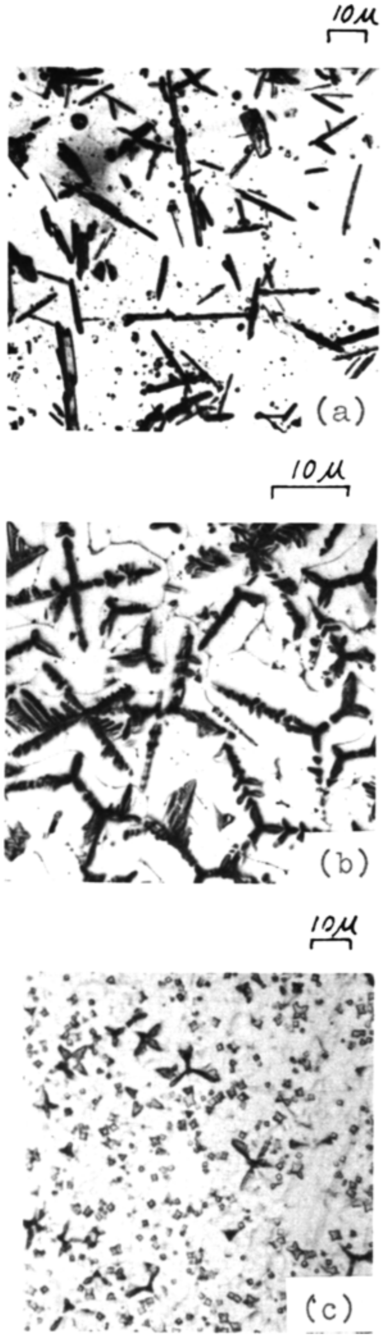

Fig. 1—Variation of microstructures of Al-Zr alloys with cooling conditions: (*a*) slow cooling and (*b*) rapid cooling of the Al-5.39 wt pct Zr alloys, and (*c*) rapid cooling of the Al-3 wt pct Zr alloys.

It is possible that the Al_3Zr phase of $L1_2$ type proposed here is a high temperature equilibrium phase above 650°C and is quenched in without transformation. To confirm it, X-ray diffraction analysis was also made on the Al-5.39 wt pct Zr alloys which were cooled rapidly from a solid-liquid coexisting temperature range. It was found that a high temperature equilibrium phase was not $L1_2$ type but tetragonal as shown in Refs. 4 to 6.

T. OHASHI and R. ICHIKAWA are Assistant Professor and Professor of Foundry Engineering, respectively, Nagoya Institute of Technology, Nagoya, Japan.

Manuscript submitted June 22, 1971.

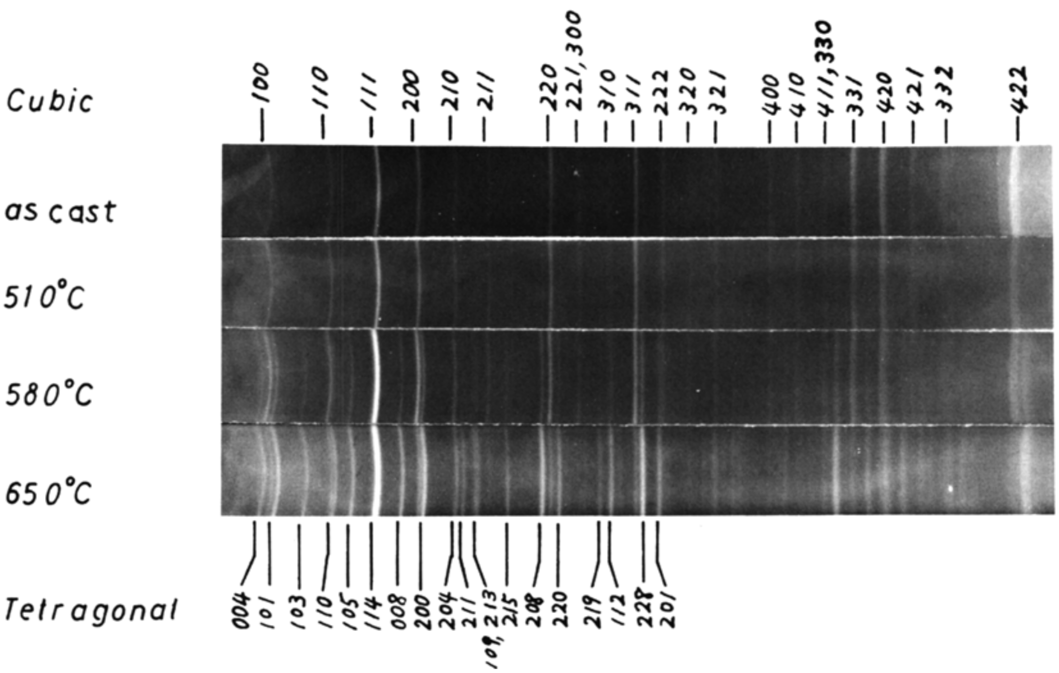

Fig. 2—Change in X-ray powder-diffraction patterns of the separated crystals by annealing temperature.

Table I. X-Ray Diffraction Lines From the Metastable Phase in the Al-5.39 Wt Pct Zr Alloys

		Intensity, I/I_{111}		
			Calculated	
d, Å	h k l	Observed	Ordered Cubic	fcc
4.037	1 0 0	s	50	–
2.879	1 1 0	m	40	–
2.351	1 1 1	vs	100	100
2.036	2 0 0	s	50	50
1.821	2 1 0	w	20	–
1.663	2 1 1	w	10	–
1.439	2 2 0	m	30	30
1.360	2 2 1 3 0 0	vw	10	–
1.290	3 1 0*	vw*	20	–
1.227	3 1 1	vw, m†	30	30
1.165	2 2 2*	vw*	10	10

*Not observed in the bulk (sheet-shaped) specimens.
†In the case of the separated powder specimens.

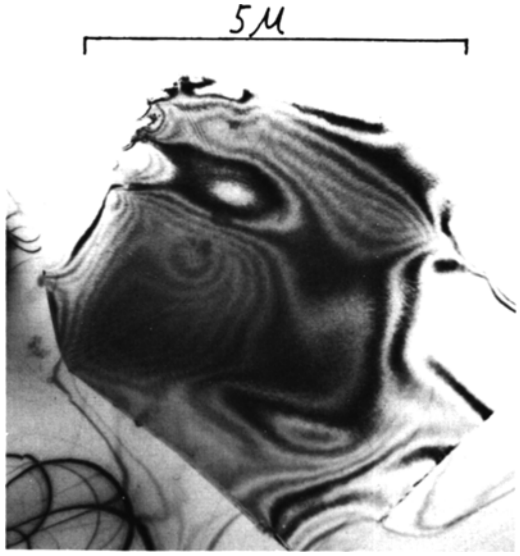

Fig. 3—Transmission electron micrograph of the thinned specimens of the rapidly solidified Al-3 wt pct Zr alloys.

A change in domain size, lattice strain and/or stacking fault density may be caused by the change in crystal structure during the transformation of the metastable phase of Al_3Zr but a measurable variation in line breath or peak shift of X-ray reflections could be hardly found by means of a diffractometer.

Fig. 3 shows transmission electron micrographs of the rapidly solidified Al-3 wt pct Zr alloys. The shape of the secondary phase observed was mostly square and like flowers with four pieces of petal, Fig. 5.

Fig. 4 shows a selected area diffraction pattern from the secondary phase. Applying the unit cell which had been previously obtained by X-ray diffraction analysis on the metastable secondary phase and knowing the structural factor, the reflections in the pattern could be identified as 200 and 220 and so forth with superlattice reflections of 100 and 110 and so forth. Thus, the secondary phase in the Al-3 wt pct Zr alloys; *i.e.*, $L1_2$ type.

Dark field image of Fig. 3 and another section of the thinned specimens are shown in Fig. 5. It was observed that the secondary phase was constructed from many fine dendritic crystals growing approximately along 100 direction. The above fact might be due to a low boundary energy between the metastable phase of Al_3Zr and the primary α solid solution.

It is interesting to note that the crystal structure of the metastable Al_3Zr phase formed by rapid solidification of the molten Al-3 ~ 6 wt pct Zr alloys is the same as that of the metastable precipitate from the supersaturated solid solutions which were obtained by rapid solidification of the molten Al-1 ~ 1.1 wt pct Zr alloys.[7]

The authors wish to thank Mr. K. Shibatomi,

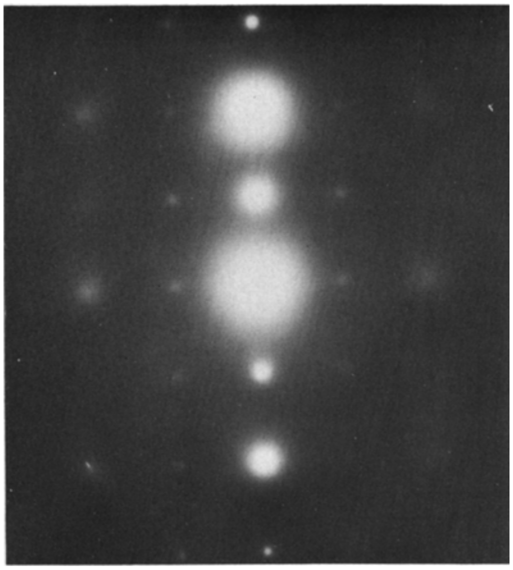

Fig. 4—Selected area diffraction pattern of Fig. 3 showing superlattice reflections of $L1_2$ type. Electron beam axis: 001.

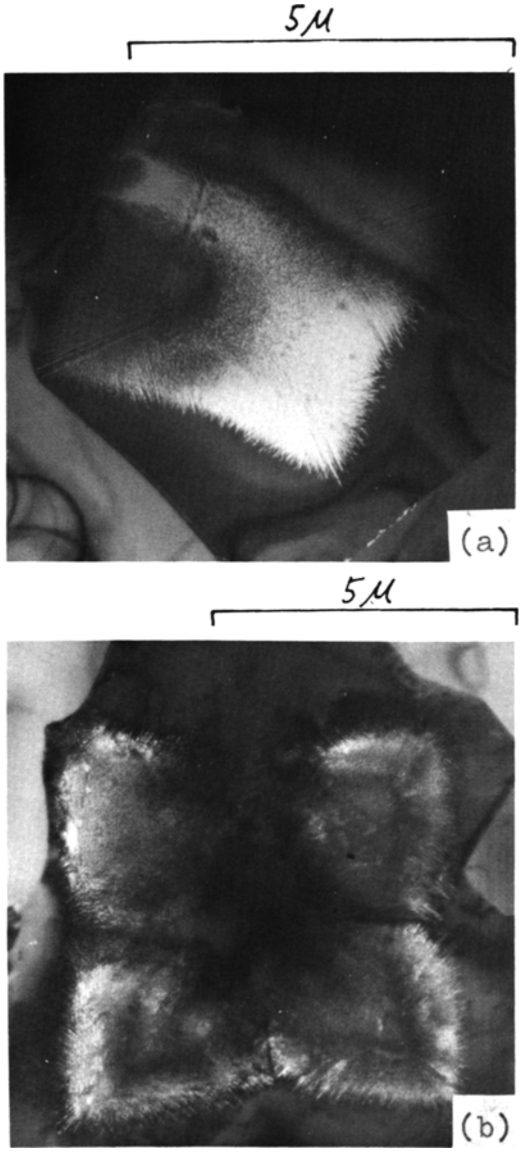

Fig. 5—Secondary phases observed in dark field images by using (100) superlattice reflection: (*a*) the same area of Fig. 4 and (*b*) another section in the specimens.

Japan Electron Optics Laboratory Co., Ltd. for operating an electron microscope device and also the Nippon Keikinzoku Co., Ltd. for supplying aluminum ingots. This research was supported in part under the Light Metal Educational Foundation, Inc., Osaka, Japan.

---

1. R. Ichikawa and T. Ohashi: *J. Japan Inst. Light Metals,* 1969, vol. 18, pp. 314-19.
2. T. Ohashi and R. Ichikawa: *J. Japan Inst. Metals,* 1970, vol. 34, pp. 604-10.
3. E. H. Hollingsworth, G. R. Frank, Jr., and R. E. Willett: *Trans. TMS-AIME,* 1962, vol. 224, pp. 188-89.
4. G. Brauer: *Z. Anorg. Allg. Chem.,* 1934, vol. 242, pp. 1-22.
5. W. L. Fink and L. A. Willey: *AIME Trans.,* 1939, vol. 133, pp. 69-80.
6. D. J. McPherson and M. Hansen: *Trans. ASM,* 1954, vol. 46, pp. 354-71.
7. O. Izumi and D. Oelschlägel: *Z. Metallk.,* 1969, vol. 60, pp. 845-51.

Cleavage in Ti-8Al-1Mo-1V Caused by Hydrogen Gas

D. A. MEYN

HYDROGEN gas causes cleavage cracking in titanium alloys under static[1-4] and cyclic[2,5,6] loading (fatigue). New observations show that such cleavage in Ti-8Al-1Mo-1V propagates in regular, minute increments under both loading conditions, on a plane 9 deg from $\{10\bar{1}0\}_\alpha$. Because stress corrosion cracking (SCC),[7,8] sustained load cracking (SLC) in inert environments,[8,9] and low amplitude corrosion fatigue cracking[10] in this alloy propagate on a markedly different set of cleavage planes (near $\{0001\}_\alpha$) without similar signs of incremental propagation, doubt is cast on the hydrogen-embrittlement mechanisms proposed to explain them.[10-13]

The starting material for the hydrogen cracking experiments was 0.265 in. thick mill annealed Ti-8Al-1Mo-1V plate.[7,10] Three single-edge-notched tensile specimens[10] were vacuum annealed, Table I, to eliminate susceptibility to SLC in vacuum, thus to more clearly register the isolated effects of H_2. R-7V1 and R-7V2 were tested in commercial ultrapurity H_2 (99.999 pct) containing <1 ppm O_2 with a dew point of -85°F, in a vacuum chamber evacuated to 1×10^{-7} torr before filling. H_2 was admitted via a stainless steel regulator and copper tubing, which had been evacuated up to the gas cylinder valve. R-7V3 was tested in a small plastic chamber through which purified H_2 flowed. The purification train included a catalytic O_2 reactor, $MgClO_4$ dryer, and liquid nitrogen trap, connected by surgical rubber tubing.

The results of cracking experiments are summarized in Table I and Figs. 1 and 2. The fracture surfaces, where H_2 cracking had occurred, were covered by a black deposit, Fig. 3, whose X-ray diffraction pattern indicates a mixture of bct, fcc, and bcc titanium hydrides. Cleavage was the pre-

---

D. A. MEYN is Research Metallurgist, Physical Metallurgy Branch, Metallurgy Division, Naval Research Laboratory, Washington, D. C.

Manuscript submitted August 16, 1971.